Optimal energy management of a mild-hybrid vehicle

Grégory Rousseau, Antonio Sciarretta, Delphine Sinoquet

OPTIMAL ENERGY MANAGEMENT OF A MILD-HYBRID VEHICLE

Gregory Rousseau [*,**] **Antonio Sciarretta** [*]
Delphine Sinoquet [*]

[*] *Institut Français du Pétrole, 1 et 4, avenue de Bois-Préau, 92852 Rueil-Malmaison Cedex - France*
[**] *Ecole des Mines de Paris*

Tel. 0033 1 47 52 63 24 / Fax. 0033 1 47 52 70 12
gregory.rousseau@ifp.fr

Abstract: The paper presents the development of a supervisory controller for a mild-hybrid vehicle, a hybrid natural gas SMART, equipped with a starter alternator and supercapacitor manufactured by Valeo. This electric additional power can be used to stop and start quickly the engine and also to power the vehicle alongside with the engine. The electric motor can also be used to recharge the supercapacitor.
After a description of the models developed for the electric motor dynamics, a dynamic programming algorithm is applied for the optimization of power split, based on these models. The resulting optimal power split is compared to a real-time control law. Among the available control laws, the choice of the Equivalent Consumption Minimization Strategy (ECMS) allows to keep the same models that have been used for dynamic programming algorithm. Moreover, some road tests show the resulting behavior of the powertrain, in terms of supercapacitor voltage, motor and engine torque and speed.

1. INTRODUCTION

Growing environmental and global crude oil supplies concerns are stimulating research on new vehicle technologies. Hybrid-electric vehicles (HEV) appear to be one of the most promising technologies for reducing fuel consumption. In this context, mild hybridization gives numerous potential advantage : (i) *(stop-and-start)* improves driving agreement by reducing noise and vibrations, (ii) the recuperation of braking energy to be stored in the battery and re-used later via the electric motor, (iii) the possibility of downsizing the engine, and (iv) the ability to choose high-efficiency engine running modes to reduce energy consumption.

The energy management of hybrid powertrains requires dedicated supervisory control laws. The controller must actually rely on the estimation of the state of charge of the energy storage system, and it must take into account the variable efficiency of each element of the powertrain. Optimization of energy-management strategies on prescribed driving cycles (offline optimization) is often used to derive sub-optimal control laws to be implemented on the vehicle (Sciarretta *et al.*, 2004), (Scordia, 2004), (Wu *et al.*, 2002), (Delprat, 2002).

Optimization tools require a mathematical description of the components of the system. In this paper, a model-based control of the propulsion system of a mild hybrid vehicle is presented. This model is used in dynamic programming algorithm, and also with a real-time ECMS-type control strategy. With respect to other implementations of this concept (Delprat, 2002), (Sciarretta *et al.*, 2004) usually adopted for battery-based parallel hybrids, here the studied powertrain includes a supercapacitor as an energy storage system. Due to its small capacity, in the normal situation, the supercapacitor is often close to its physical voltage limits. That is a major difficulty when using real-time control, which deserves particular techniques detailed in the following.

2. SYSTEM MODELLING

IFP has developed a mild hybrid vehicle, equipped with a natural gas engine, a reversible starter-alternator, and a supercapacitor (Valeo Starter Alternator Reversible System, StARS). (Tilagone and Venturi, 2004). The partners of this project are Gaz de France, INRETS and Valeo, with financial support by ADEME.

The resulting architecture is a mild-hybrid powertrain: the torque requested for traction cannot be provided by the electric motor only. Thus, the engine cannot be turned off, except during idling (*stop-and-start*). The electric motor can be controlled by several modes:

(1) the boost mode, where the electric motor provides a traction power alongside with the engine;
(2) the regenerative mode, where
   a the motor is used as a generator to decrease vehicle speed and recharge the supercapacitor (regenerative braking), or
   b the generator drains an extra power from the engine (torque defined by energy management);
(3) the alternator mode, where a constant supercapacitor voltage setpoint is imposed (typically 16.2 V); this mode is only used when the voltage drops below a certain threshold.

In the following, the electric power required by the auxiliaries (supply of electric power for lights, vehicle control unit, etc.), and drained from a 14 V auxiliary battery is taken into account as well. However, for simplicity, we assume that it is the supercapacitor that provides the electric power (via the DC/DC module) to maintain the battery voltage at 14 V. We also assume that the requested power is constant at 140 W.

In order to optimize the energy management of the VEHGAN, either a quasistatic backward model is used, or a more detailed AMESim model (Dabadie *et al.*, 2005) to calculate the speed $\omega_{rq}(t)$ and torque $T_{rq}(t)$ required at the engine output shaft along a prescribed drive cycle. This torque request can be split between the engine torque $T_e(t)$ and the electric motor torque $T_m(t)$. Finding the optimal splitting strategy is the objective of the supervisory controller. To evaluate the performance of the two components as a function of their respective torque, a simplified model of the system is built, which consists of:

- a model of the 0.660 l natural gas engine; the engine performance is characterized by the fuel consumption map displayed in Figure 1 and by its maximum torque $T_e^{max}(\omega_{rq})$ that depends on the engine speed, see (13),
- a model of the 3 kW starter-alternator (described in section 2.1.1),
- a model of the supercapacitor, which is made up of 12 modules of 1500 F; this model is described in section 2.1.2.

2.1 Submodels of the electric components

All the models described in the following section are taken from (Rousseau *et al.*, 2007). To model the electric motor in a realistic way, two different models depending on the sign of the power are considered. If the delivered power is positive, then the electric motor is used to provide some additional power to the engine, and the torque is positive. Otherwise, when the electric motor is used as a generator, maps provided by the manufacturer are used, which give the delivered current as a function of voltage, speed, and torque.

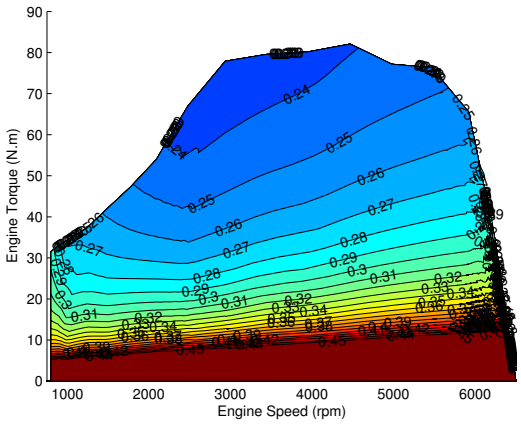

Fig. 1. Fuel consumption map of natural gas engine of VEHGAN vehicle

2.1.1. Electric motor The starter–alternator used in the VEHGAN vehicle is a permanent-magnet motor with six magnets.

To limit the complexity of the model, the motor is modelized using DC motor equations by neglecting the non-linear contribution:

$$T_m(t) = \frac{1}{R_a}(K_m(t)U_a(t) - K_a(t)K_m(t)\omega(t)), \tag{1}$$

where $\omega(t)$ is the motor speed, $U_a(t)$ plays the role of the DC armature voltage,

$$U_a(t) = K_a(t)\omega(t) + R_a I_a(t), \tag{2}$$

$I_a(t)$ plays the role of the armature current, R_a of the armature resistance.

The quantities $K_a(t)$ and $K_m(t)$ are not constant as in DC motors, since they represent influence of the variable d,q voltages and currents performed by the motor controller.

2.1.2. Supercapacitor A simple equivalent circuit of a supercapacitor consists of a capacitor and a resistor in series (Sciarretta *et al.*, 2004). The Kirchhoff's voltage law yields

$$U_s(t) = \frac{Q(t)}{C} - R_s I_s(t), \qquad I_s(t) = -\frac{dQ(t)}{dt}, \tag{3}$$

where $U_s(t)$ is the terminal voltage, $I_s(t)$ is the terminal current, R_s is the equivalent resistance, C is the capacitance, and $Q(t)$ is the charge.

2.1.3. DC/AC Link The electric power link between electric motor power P_a and supercapacitor power P_s is achieved with an inverter. We assume here that the motor torque is controlled by the voltage ratio $\lambda(t)$ of the inverter:

$$U_s(t) = \frac{1}{\lambda(t)}U_a(t), \qquad I_s(t) = \lambda(t)I_a(t). \tag{4}$$

Because of internal physical constraints, it is not possible to control the electric motor with a continuous control variable $\lambda(t)$ when positive torque is requested (boost mode). Instead, five discrete values of λ are available at each time t, as a function of the system operating conditions. This discrete controller permits to obtain five values of boost torque, depending on the supercapacitor voltage and the motor speed. The difference between minimum and maximum available torques does not exceed 2 Nm. In regenerative mode, however, it is possible to control the electric motor with a continuous λ, meaning that all admissible regenerative torques are available.

2.2 Dynamic model of the whole electric system

The physical causality representation of the whole electric system is sketched in Figure 2. The speed is an input variable, together with the controller λ. The torque is the output variable.

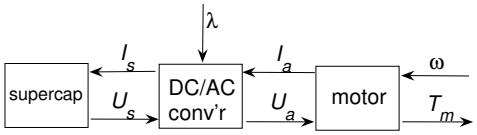

Fig. 2. Dynamic representation of the electric system

To obtain the dynamic dependency between torque and speed, we differentiate each term of (3), which leads to

$$\dot{U}_s(t) = -\frac{I_s(t)}{C} - R_s \dot{I}_s(t). \tag{5}$$

From (2) and (4) we obtain

$$I_s(t) = \lambda(t)\frac{\lambda(t)U_s(t) - K_a(t)\omega(t)}{R_a}. \tag{6}$$

From (5) and (6) we finally obtain

$$\begin{aligned}\dot{U}_s(t) \;=\; & \frac{\lambda(t)}{1+\lambda(t)^2\frac{R_s}{R_a}}\Big[-\frac{\lambda(t)U_s(t) - K_a(t)\omega(t)}{CR_a} \\ & + \frac{R_s}{R_a}K_a(t)\dot{\omega}(t)\Big].\end{aligned} \tag{7}$$

The model given by (7) is validated against boost measurements (see (Rousseau *et al.*, 2007)) taken on a dedicated test bench at Valeo. Figure 3 shows the transient behavior of the supercapacitor voltage resulting from a motor speed step occurring in the first seconds of test. The experimental data are post-processed with a filter having a time constant of about 100 ms. Four speed levels are shown in the figure, ranging from 3000 rpm to 6000 rpm. Starting from an initial open-circuit value of 24 V, the supercapacitor voltage exhibits an abrupt drop of about 4 V, followed by a slower decrease. Consequently, the supercapacitor current (not represented) exhibits an initial rise, appearing as a smooth peak due to the low-pass filtering, followed by a slower decrease that would virtually end when the supercapacitor is completely discharged.

The comparison between experimental data and simulations of Figure 3 shows that the simplified approach of (7) is indeed able to represent the main dynamics of the system. The control parameters K_a and K_m have been parameterized as

$$K_a = \frac{K_{a0}}{\omega(t)}, \qquad K_m = K_{m0}\frac{U_s(t)}{\omega(t)}. \tag{8}$$

The tests of Figure 3 were performed for a given setting of the discrete motor controller. In the simulations, that corresponds to a specific value λ_4 of the voltage ratio of the inverter. For the specific value λ_4, the simulation results can be compared to experimental data.

To model the regenerative mode behavior, instead of using (7), we replace the DC/AC model and the electric motor model by a map provided by Valeo. Equation (6) is then replaced by the following

$$I_s(t) = f(U_s(t), \omega(t), T_m(t), \tag{9}$$

where $f(\cdot)$ corresponds to the map depending on speed ω, voltage U_s, and torque T_m. The motor torque is calculated as matching exactly the torque setpoint T_m°, which thus substitutes λ as an input variable to the motor/converter submodel, see Figure 2.

The overall model has been implemented in Matlab Simulink, and used within a dynamic programming algorithm.

3. DYNAMIC PROGRAMMING OPTIMIZATION

3.1 Optimal Control Problem

The optimal control problem under study consists in minimizing the fuel consumption of the vehicle along a prescribed driving cycle, while providing charge sustenance to the supercapacitor, and taking into account physical limits of the supercapacitor, the engine, and the electric motor.

We define the control variable $u(t)$ which represents the split factor of the requested torque T_{rq}, between the engine torque T_e and the motor torque T_m:

$$\begin{cases} T_{rq}(t) = T_e(t) + \rho T_m(t) \\ T_e(t) = u(t)T_{rq}(t) \end{cases}, \tag{10}$$

where ρ corresponds to the ratio between electric motor speed and engine speed, $\rho = \omega(t)/\omega_{rq}$. This ratio is equal to 1.96 on the studied vehicle.

The only relevant dynamics considered is that of supercapacitor voltage, called $U(t)$ in the following

$$\dot{U}(t) = f(U(t), u(t), t). \tag{11}$$

The resulting optimization problem is then the following :

$$\begin{cases} \min\limits_{u \in W(t)} \left\{ J(u) = \int\limits_0^T L(u(t),t)dt + g(U(T),T) \right\} \\ \text{subject to : } \; \dot{U}(t) = f(U(t),u(t),t), \;\; U(0) = U_0 \end{cases} \tag{12}$$

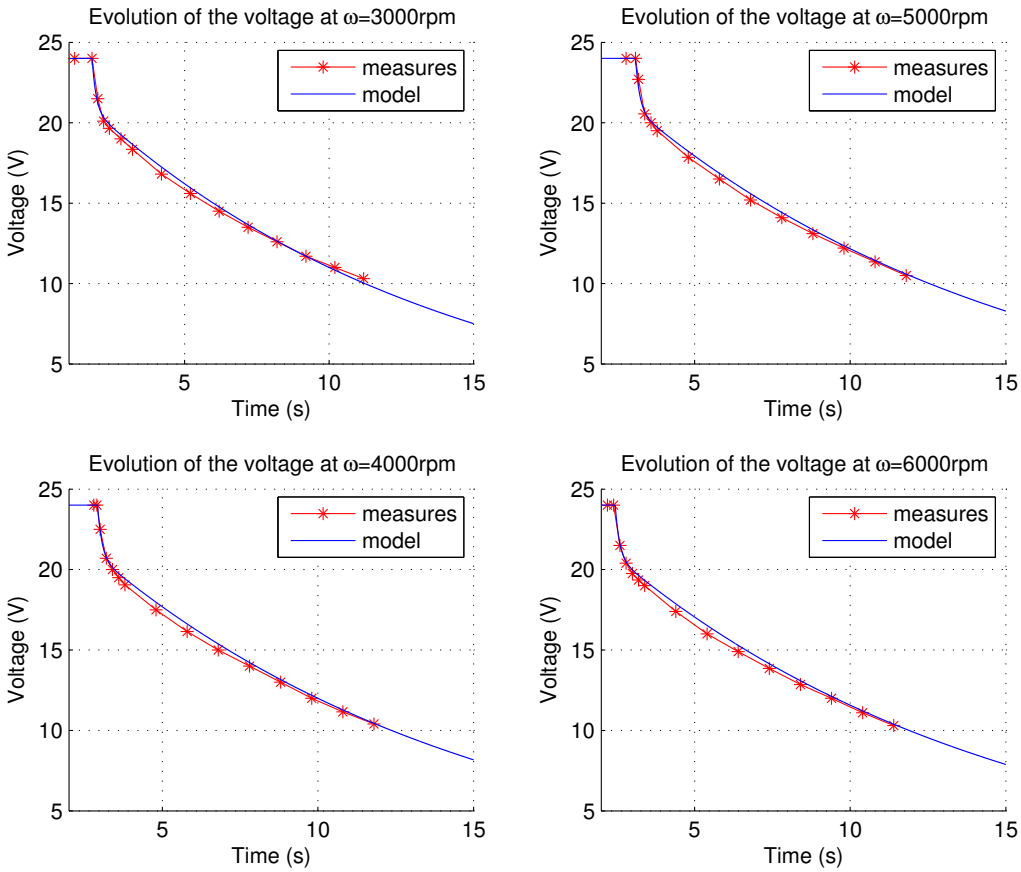

Fig. 3. Experimental data compared to model: evolution of the voltage $U_s(t)$

where T is the final time of the drive cycle, $L(u(t),t)$ is the fuel consumption rate, computed from the data displayed in Figure 1, $g(U(T),T)$ is a term that penalizes any deviation of the final voltage from the initial voltage.

In addition to the latter "soft" constraint over the final state, the problem (12) is also subject to the following inequality constraints, leading to the feasible control space $W(t)$:

- the engine can only produce a positive torque, which is limited to a maximum torque that depends on engine speed $\omega_{rq}(t)$, leading to the control constraints

$$0 \leq u(t)T_{rq}(t) \leq T_e^{max}(\omega_{rq}(t)), \tag{13}$$

- the electric motor torque is limited between a maximum torque and a minimum torque during regenerative mode, leading to the control constraints

$$\begin{aligned} \rho T_m^{min}(\omega(t)) \leq (1-u(t))T_{rq}(t) \\ \leq \rho T_m^{max}(\omega(t)), \end{aligned} \tag{14}$$

- the motor controller, during boost mode, can only be set to one over five discrete values, thus

$$\lambda(t) \in (\lambda_i)_{i\in[\![0,4]\!]}, \tag{15}$$

as already discussed; that also leads to corresponding control constraints on the allowed positive torques.

The state variable is also subject to inequality constraints, deriving from physical limits of the supercapacitor and of the motor,

$$U_{\min} \leq U(t) \leq U_{\max}. \tag{16}$$

The values of $U_{\min}$ and $U_{\max}$ are set to 16 V and 24 V respectively.

3.2 DP Optimization algorithm

The Dynamic Programming method (DP) is usually used to solve the problem (12) ((Wu *et al.*, 2002), (Scordia, 2004)). It relies on the principle of optimality or Bellman principle. First, the optimal control problem (12) is discretized in time

$$\begin{cases} \min\limits_{u_k\in W_k} J(u) := \sum\limits_{k=0}^{N-1} L_k(u_k) + g(U_N) \\ \text{subject to :} \quad U_{k+1} = f_k(U_k,u_k), \quad U(0) = U_0 \\ U_{\min} \leq U_k \leq U_{\max} \end{cases} \tag{17}$$

where $L_k(u_k)$ is the fuel consumption over the time interval $[k,k+1]$, U_k is the voltage of the supercapacitor at time k, f_k

is the function (11) at time k, and $g(U_N) = \beta(U_N - U_0)^2$ is the penalization term (β is a constant to be chosen), N is the final time, W_k the feasible domain for u_k with respect to constraints (13), (14), and (15).

From Bellman principle, the cost-to-go function $V_k(x_k)$ at the time step k, $0 \leq k \leq N-1$, is expressed as

$$V_k(U_k) = \min_{u_k \in W_k} (L_k(u_k) + V_{k+1}(f_k(U_k, u_k))). \quad (18)$$

At time N, the cost-to-go is $V_N(U_N) = g(U_N)$.

This optimization problem is solved backward from final time step to initial time step using a discretization of function V in the control space and in the state space. A description of the classical DP algorithm can be found in (Bertsekas, 2001), we refer to (Guilbaud, 2002) for some theoretical results on the convergence and error estimations.

In the following, the control u is specialized as the feasible λ values in boost mode, and by the torque setpoint T_m° in regenerative mode.

3.2.1. Model implementation A tool developed by IFP, based on dynamic programming, has been used to solve the optimization problem. The general outline of the optimization tool is described in Figure 4. It allows to plug any vehicle and powertrain model with the dynamic programming algorithm.

Each control u_k of the electric motor is tested for each point of the discretization grid (t_k, U_k). As for a real-time controllers, operating conditions will forbid some or all the values of the control. The tested controls are then really applied only if these are feasible controls. Otherwise, the electric motor can not be used. Figure 5 represents the tested controls on a particular operating point. Eleven control values are tested, with five positive torques (corresponding to the feasible values of λ), five negative torques (arbitrarily chosen among feasible regenerative torque values) and one last value where the electric motor is not used.

The model, executed at time t_k, provides the instantaneous fuel consumption L_k and the variation of the state, U_{k+1}, for each control u_k. Finally, the DP algorithm selects the optimal control u^* according to (17).

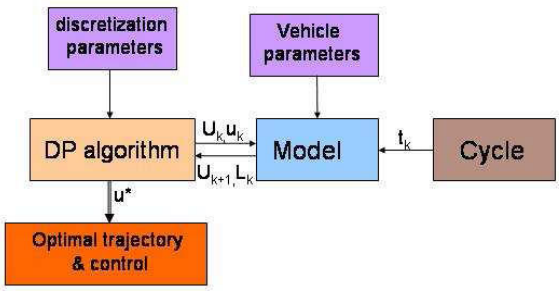

Fig. 4. Diagram of the optimization tool

A standard time step used in our examples, for dynamic algorithm, is 1 s. However, the time step of the Simulink model can be smaller than the dynamic programming one. Considering a smaller time step for the dynamic model permits to limit approximation errors, and to calculate a more realistic variation of voltage over a time step. In our model, the chosen time step is 0.1 s.

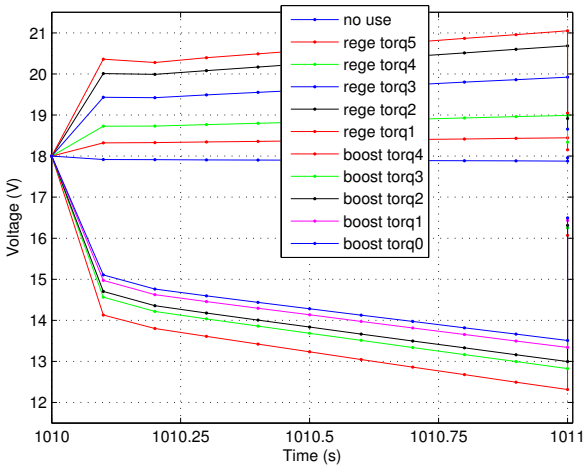

Fig. 5. Evolution of voltage trajectories along a time step with different controls.

3.3 Optimization Results

To calculate fuel consumption over a whole driven cycle, we use a additional matlab model, which gives exact wheel speed and torque corresponding to the vehicle parameters. The optimal system trajectories are calculated for the NEDC cycle, and shown in Figures 6 and 7.

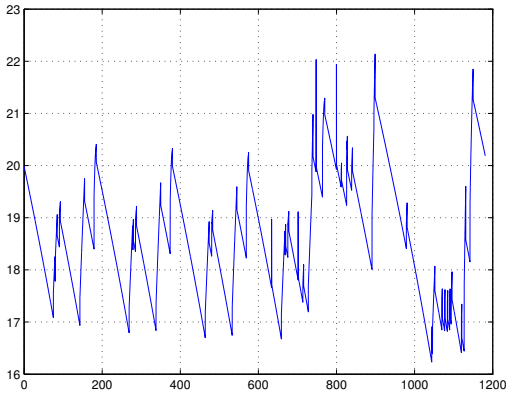

Fig. 6. Optimal trajectory of the supercapacitor voltage

Figure 6 clearly shows that the final voltage constraint is approximately verified. The electric energy delivered by the supercapacitor to feed the auxiliaries (constant-rate voltage decreases) is compensated by the energy recuperated either from regenerative braking or via the engine (generator mode). Because of the low global efficiency (≈ 0.80) of the electric system and of the large number of constraints, notably the only

five allowed torques when boost is required, boost is never selected as an option. This particularity is also a consequence of the fact that the vehicle is able to follow the NEDC cycle without any need of a secondary power source to help the engine.

Figure 7 shows the transient behavior of supercapacitor voltage. Each time a regeneration is applied, the supercapacitor voltage exhibits a rise followed by a constant-rate increase. A voltage drop then ends the regeneration phase.

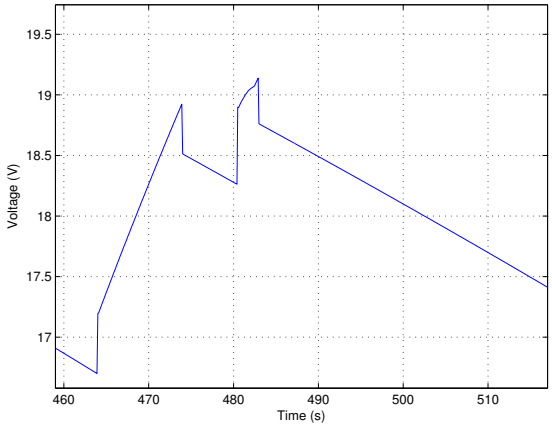

Fig. 7. Optimal trajectory of the supercapacitor voltage (zoom)

Quantitative results of DP vary according to the level of complexity used to represent the auxiliary power needs and torque demand from the driver. Improvements in fuel consumption obtained with hybridization range around 1% of the fuel consumption for a baseline case. In the latter, the engine only drives the vehicle while the motor uses regenerative braking to drive the auxiliaries.

Thus, accordingly to the DP results, energy management seems not much helpful in reducing the fuel consumption. However, these results must be put into perspective. First, the *stop-and-start* has not be taken into account in the offline optimization. This functionality should lead to interesting fuel consumption reduction. Moreover, the most *stop-and-start* is used, the most the energy management will be helpful to recharge and maintain a correct supercapacitor voltage, and to optimize fuel consumption. Second, some improvements on the electric models must be carried on. Basically, because of internal temperature constraints inside the electric motor, the real boost torque is smaller than the boost torque given by the model. As a consequence, during simulations, the boost mode could be applied only on few operating points, when done on NEDC cycle. Finally, the initial aim of adding an electric motor to this vehicle is to maintain the same functionalities of a conventional Smart, by using a downsized engine coupled with a starter-alternator. In this perspective, the energy management become an interesting add-on to decrease much more the fuel consumption.

4. REAL-TIME FEEDBACK CONTROL

4.1 ECMS

In this section, suboptimal control law is derived from the optimization results. The chosen real-time control law is the Equivalent Consumption Minimization Strategy (ECMS): it is based on instantaneous equivalent fuel consumption. The battery is considered as a second energy source, and ECMS aims to choose the cheapest energy source, between fuel tank and battery storage. To do so, we form the Hamiltonian function $\mathcal{H}$ given by:

$$\mathcal{H} = \dot{m}\Delta t + p\dot{E}_{elec}\Delta t, \tag{19}$$

where $\dot{m}\Delta t$ represents the variation of fuel consumption over a time step, and $\dot{E}_{elec}\Delta t$ corresponds to the variation of electric energy of the supercapacitor over a time step. In this strategy, the optimal control is the admissible one which minimizes $\mathcal{H}$, taking into account all constraints. The same models as the ones used in dynamic programming algorithm are here used in ECMS.

4.2 Meaning of p (Lagrange multiplier)

The coefficient p corresponds to the *price* of electric energy. The larger is p, the more expensive is the electrical energy, and the more interesting to be recovered. The smaller is p, the cheaper is the electrical energy, and the more interesting to be used to power the vehicle conjointly with the engine. Some values of p corresponds to situations where it is better to just use the engine without any help of electric motor.

The variation of p depends on the time evolution of the dynamic state variable, according to the Euler-Lagrange equations. While for batteries the state variable is usually the charge, the supercapacitor state is rather in terms of voltage U. However, using simply U as the state, as done in section 3.2, would imply that $\dot{U}$ varies with U for a given electric power. This would result in an accordingly varying p.

The energy stored in the supercapacitor, $E_{elec} = \frac{1}{2}CU^2$ is chosen as a state instead, with a dynamic state equation

$$\dot{E}_{elec} = CU\dot{U}. \tag{20}$$

With this choice, which also justifies the form (19) of the Hamiltonian, p is ideally a constant. However, this is no longer true in the presence of active state constraints. Thus, p must be determined along the cycle.

4.3 Determination of p

The determination of p is an open question, and the initial value of p, p_0, at the beginning of the cycle, is much more difficult to know. Many authors (Liu and Peng, 2006), (Delprat, 2002) control p as a linear function of state of charge or considerer dependance with other measurements. Even if this

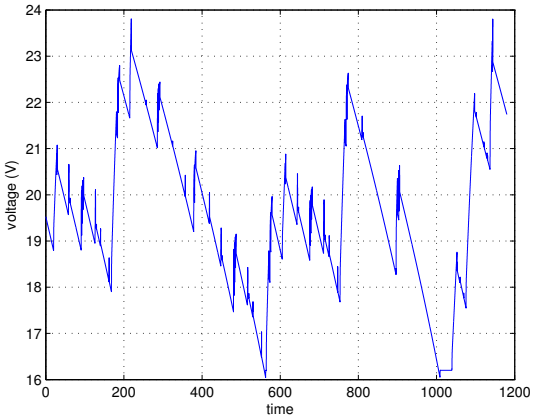

Fig. 9. Sub-optimal voltage with ECMS

choice is quite well-founded to be used in a real-time strategy, it is not optimal. However, it permits to enhance the regeneration phases when state of charge is low.

An adequate initial value can be obtained by calculating the equivalent Lagrange multiplier when using the dynamic programming results. From (Bryson and Ho, 1975) equivalence between Pontryagin's maximum principle and dynamic programming can be showed if

$$p(t) = \frac{1}{U}\frac{\partial V}{\partial U}(t,U), \tag{21}$$

where $V(t,U)$ corresponds to the cost-to-go function in continuous time, already defined in (18). The term $\frac{1}{U}$ appears here because of the difference of variation taken into account: ΔU in dynamic programming, but $U\Delta U$ in ECMS.

In the following, we consider that p remains constant as long as the supercapacitor voltage trajectory stays between allowed limits, 16 V et 24 V. Previous work of the authors (Rousseau *et al.*, 2006) and (Rousseau *et al.*, 2008) has shown the behavior of p when the state touches a boundary, in simpler optimization problems. However, the optimal trajectory of p can be very complex, as it depends on the dynamics (11) and also on the future active state constraints. Therefore, p is controlled by an integrator as long as the voltage U goes beyond given voltage limits.

4.4 Simulation results

The control law described above has been implemented in a complete vehicle model. To do so, we use the co-simulation between an AMESim model, and the Simulink controller. The Simulink controller includes the control of all the engine actuators, and corresponds to the one that is used on vehicle. The model, which can be seen on Figure 8, reproduces all the main dynamics of the vehicle and of the powertrain. This model, including a description of the vehicle, has already been described in (Tona *et al.*, 2007).

Figure 9 clearly shows that the electric motor is only used to recharge the supercapacitor, and that the boost is never used. The main constraints on positive torques (only five possible controls) does not allow the electric motor to be used as a boost. Basically, the torque provided by the electric motor, as it has been considered in the model, would decrease the engine torque of about 25 Nm to 30 Nm at low engine speed, which is a high value compared to the potential of the vehicle. This consideration, coupled with global efficiencies of electric motor of about 80% are enough to explain the results obtained. Between time $t = 1000$ s and $t = 1040$ s, the alternator mode, corresponding to a simple voltage sustaining at $U = 16.2$ V, is active.

Table 1. Sub-optimal fuel consumption values

Th. mode	Th. mode & brake recup. (baseline)	E.M.
458 g	454.1 g	452.7 g

The fuel consumption results are indicated in Table 1. The thermic mode result corresponds to the fuel consumption obtained with the conventional powertrain, without regenerative braking. In this configuration, the engine is used to yield the requested power for the auxiliaries, via the starter-alternator. The second result corresponds to fuel consumption obtained while considering the previous, and the recovered energy from braking situations (the baseline in (3.3)). In normal driving conditions, the voltage decreases until the alternator gives the requested power as to maintain the voltage. The third results gives fuel consumption obtained with energy management (E.M.). In this strategy, the controller chooses the best moment to regenerate the supercapacitor thanks to the engine, instead of using the alternator mode all the time. Although the fuel consumption gain is not significant, this strategy allows to store some electric energy that can be reused later for the boost.

4.5 Vehicle results

The implemented control law has been successfully tested on the vehicle, and the correct behavior of supercapacitor voltage has been observed. Figure 10 shows the results obtained by testing the vehicle on a short portion of road. The decrease of the voltage due to the auxiliaries, which is quite high in this test because of the prototype system to be powered, is clearly observed. The variation of p remains constant while the voltage stays within 16.5 V and 23.5 V, which are its target bounds. When the voltage crosses these limits, the energy management controls p thanks to an integrator, as to decrease p and to change the price of electric energy. It should be noticed that, due again to the small energy stored in the supercapacitor, the system is very sensitive even to very small variations of p, as those shown in the figure. The electric motor torque setpoints are also represented in Figure 10 with some regenerative braking (here, the torques are limited to -4 Nm) during vehicle decelerations, which corresponds to null engine torque (fuel cut-off). The last braking, between $t = 50$ s and $t = 51$ s, does not allow to regenerate, as the supercapacitor voltage is still above its limit of 23.5 V. The energy management also controls both engine and electric

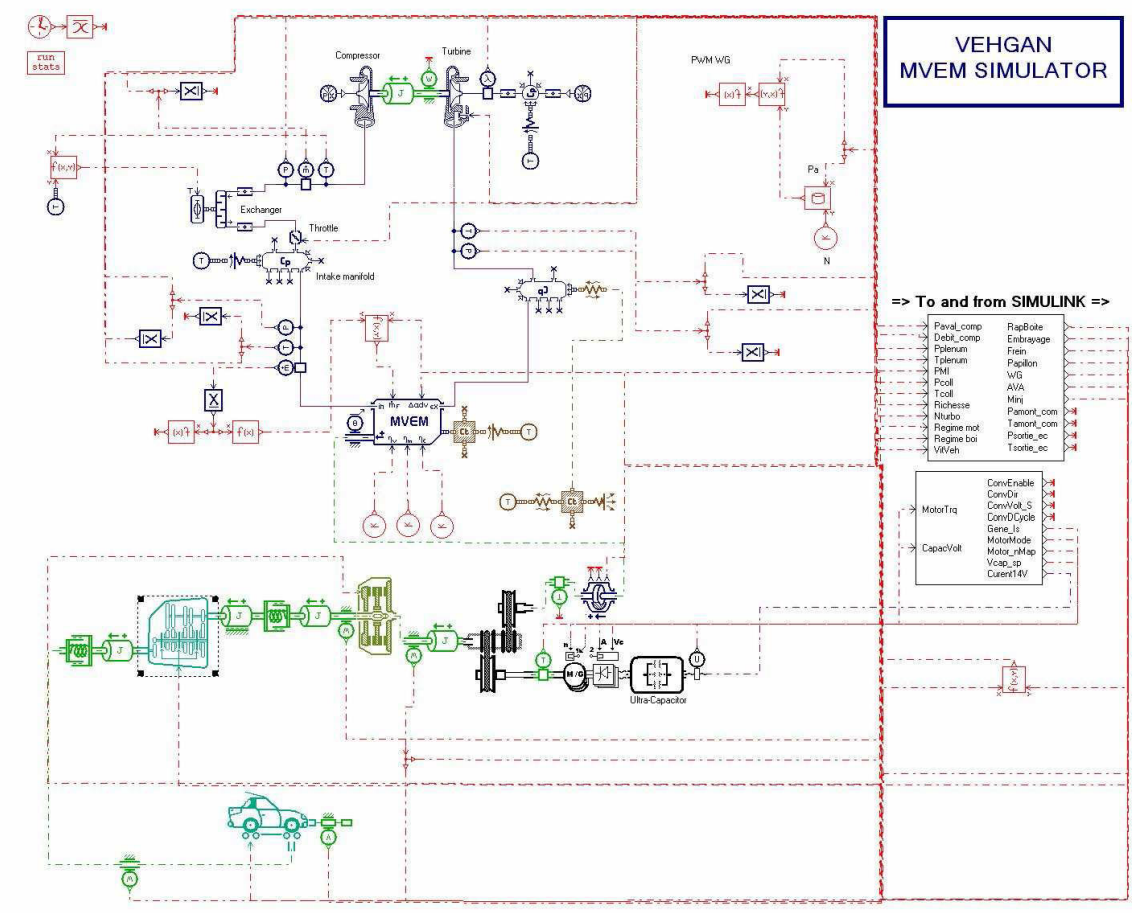

Fig. 8. AMESim model used in co-simulation

motor to recover some electric energy, see time $t = 30$ s and $t = 42$ s, by increasing the engine torque, with respect to the driver torque, to increase engine efficiency. In this plot, the driver torque corresponds to the sum of the engine torque and the electric motor torque, $T_e = T_{rq} - \rho T_m$.

The last plot of Figure 10 shows that the engine speed is not affected by the starts and the stops of the electric motor.

5. CONCLUSIONS

In this paper, has been presented a model-based of a mild hybrid vehicle. The model is based on physical equations of a DC electric motor, a supercapacitor, and an inverter. The model parameters have been successfully fitted to experimental data in order to simulate accurately the behavior of the electric system.

This dynamic model has been used in a dynamic programming algorithm to minimize the fuel consumption, taking into account the main physical constraints of the system (especially the discrete control settings).

The same models have been used to build an energy management controller, based on ECMS. The key parameter, the Lagrange multiplier p has been pre-established from dynamic programming results.

The first results, experimental and simulation, show that the room left for energy management in reducing the fuel consumption is rather limited. That is manly due to two reasons: (i) the supercapacitor, while sufficient for improving acceleration performance through boosting or allowing some regenerative braking due to its rather good power has a limited energy to act properly as a buffer; (ii) the stop-and-start capability has not been taken into account in the optimization, in order to focus only on the energy flows during traction phases.

The stop and start functionality, which allows to turn off the engine at idles, will also have a great impact on fuel consumption, and the availability of the electric power necessary to turn on the engine can also be optimized thanks to energy management.

Future work will therefore include some improvements on the models and some additional tests on the vehicle to explore the real potential of energy management.

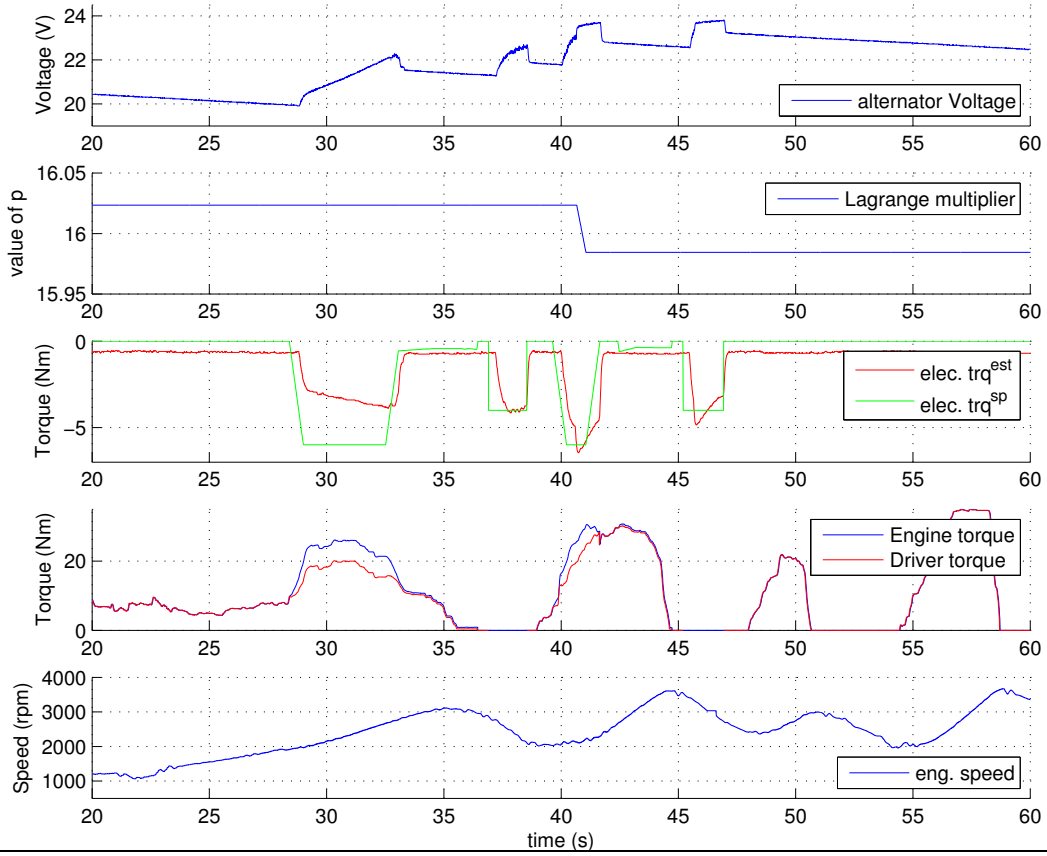

Fig. 10. Evolution of voltage, p, torques, and speed during a road test

REFERENCES

Bertsekas, D.P. (2001). *Dynamic programming and optimal control*. Vol. 1. Athena scientific.

Bryson, E. and Y.C. Ho (1975). *Applied Optimal Control*. Hemisphere Pub. Corp.

Dabadie, J.C., P. Menegazzi, R. Trigui and B. Jeanneret (2005). A new tool for advanced vehicle simulations. *ICE - International Conference on Engine for Automotive, 7th, Capri*.

Delprat, S. (2002). Evaluation de stratégies de commande pour véhicules hybrides parallèles. PhD thesis. Université de Valenciennes et du Hainaut-Cambresis.

Guilbaud, T. (2002). Méthodes numériques pour la commande optimale. PhD thesis. Université de Paris VI.

Liu, J. and H. Peng (2006). Control optimization for a power-split hybrid vehicle. *2006 American Control Conference, Minneapolis, USA*.

Rousseau, G., A. Sciarretta and D. Sinoquet (2006). Hybrid electric vehicles : From optimization toward real-time control strategies. *First Workshop on Hybrid and Solar Vehicles, Salerno, Italy*.

Rousseau, G., A. Sciarretta and D. Sinoquet (2007). Real-time control srategies for hybrid vehicles issued from optimization algorithm. *4th Symposium Hybrid Vehicles and Energy Management, Braunschweig*.

Rousseau, G., Q. H. Tran and D. Sinoquet (2008). Scop : a sequential constraint-free optimal control problem algorithm. *2008 Chinese Control and Decision Conference (2008 CCDC), Yantai, China*.

Sciarretta, A., L. Guzzella and M. Back (2004). A real-time optimal control strategy for parallel hybrid vehicles with on-board estimation of the control parameters. *Proceedings of IFAC Symposium on Advances in Automotive Control AAC04* pp. 502–507.

Scordia, J. (2004). Approche systématique de l'optimisation du dimensionnement et de l'élaboration de lois de gestion d'énergie de véhicules hybrides. PhD thesis. Université Henri Poincaré - Nancy 1.

Tilagone, R. and S. Venturi (2004). Development of natural gas demonstrator based on an urban vehicle with a downsized turbocharged engine. *Oil and Gas Science and Technology* **59**(6), 581–591.

Tona, P., P. Moulin, S. Venturi and R. Tilagone (2007). Amt control for a mild-hybrid urban vehicle with a downsized turbocharged cng engine. *SAE 2007 World Congress, Detroit*.

Wu, B., C-C. Lin, Z. Filipi, H. Peng and D. Assanis (2002). Optimization of power management strategies for a hydraulic hybrid medium truck. *Proceeding of the 2002 Advanced Vehicle Control Conference, Hiroshima, Japan*.

ACKNOWLEDGMENTS

We would like to thank Paolo Tona and Rachid Amari for their help and for the time spent during the tests on vehicle. We also acknowledge Dominique Soleri to let us quite free to test our strategy on the VEHGAN vehicle. We would like to thank Pierre Rouchon for helpful discussions and advice at various stages of the elaboration of this work.